

Iron and cobalt silicide catalysts-assisted carbon nanostructures on the patterned Si substrates

Hui Lin Chang*, Chao Hsun Lin, Cheng Tzu Kuo

Department of Material Science and Engineering, National Chiao Tung University, Hsinchu 300, Taiwan, ROC

Abstract

Catalyst-assisted carbon nanotubes (CNTs) and carbon nano-rods were synthesized on the patterned or un-patterned Si wafer by microwave plasma chemical vapor deposition, using iron or cobalt silicide catalysts. Controllable carbon nanostructures were achieved by manipulating carbon and nitrogen concentration in the source gases, catalyst materials, and patterned wafer application. CNTs were synthesized under a high ratio of $\text{CH}_4/\text{H}_2=0.1$, while carbon nano-rods were synthesized under a low ratio of $\text{CH}_4/\text{H}_2=0.01$. Introducing N_2 gas into CH_4/H_2 source gases gives rise to bamboo-like CNTs formation. Selective CNTs depositions were applied on (a) parallel Fe-coated line arrays, (b) CoSi_x -coated hole arrays. This is a novel method that is compatible with Si microelectronic device manufacturing. The field emission results indicate that the emission current density can be above $1 \text{ mA}/\text{cm}^2$ at $3.97 \text{ V}/\mu\text{m}$, and hollow like CNTs belong to better emission current than bamboo-like CNTs. Growth models of different carbon nanostructures are proposed.

© 2002 Elsevier Science B.V. All rights reserved.

Keywords: Carbon; Field emission; Chemical vapor deposition; Catalysis

1. Introduction

Carbon nanotubes (CNTs) that consist of sheet(s) of graphite (a hexagonal lattice of carbon) rolled into a cylinder, were discovered in 1991 by Iijima [1]. This novel material has inspired much excitement in recent years and a large amount of research has been dedicated to their understanding. Mechanically, the axial Young's modulus of multi-walled CNTs can be as high as 1800 GPa, and the tubes can thus be much stiffer than commercial carbon fibers [2]. Electrically, the tubes are either metallic or semiconducting depending on their chirality [3,4]. Chemically, the tubes are inert and highly resistant to oxidation [5]. The unique properties of CNTs are also predicted to possess a great potential in applications of scanning probes [6], field emission (FE) display [7], anode for lithium ion batteries [8], nano-electronic devices [9], supercapacitors [10], molecular sensors [11] and hydrogen storages [12].

The goals of CNTs synthesis can be considered to be CNTs with highly ordered orientations, fewer defects and reproducibly controllable properties. Chemical vapor

deposition (CVD) method offers advantages of controlling CNT orientations and properties, by varying synthesis parameters and substrate pretreatment. For example, an enhanced CVD approach can obtain directionally suspended SWNTs networks in which the SWNTs are aligned and parallel to the substrate [13]. Also, CVD methods can be used to obtain various kinds of CNTs, such as CNTs with a perfect Y-junction or straight line, bridging CNTs on two parallel patterned structures, the selective, lateral growth of bamboo-like CNTs [14,15].

This study systematically explores the carbon nanostructures synthesized by microwave plasma CVD (MPCVD) with various compositions and ratios of source gases. The novel catalyst of CoSi_x , much employed as a contact and as gate electrode films for Si microelectronic devices, is used, and Fe catalyst is used for comparison. The selective growth of CNTs on parallel line arrays, and hole arrays is also explored. Growth models of different carbon nanostructures are proposed.

2. Experimental

CNTs and carbon nano-rods were synthesized on Si wafers and patterned Si wafers with parallel line arrays

*Corresponding author. Tel.: +886-3-5739845; fax: +886-3-5724727.

E-mail address: gladies@mail.mayju.com.tw (H.L. Chang).

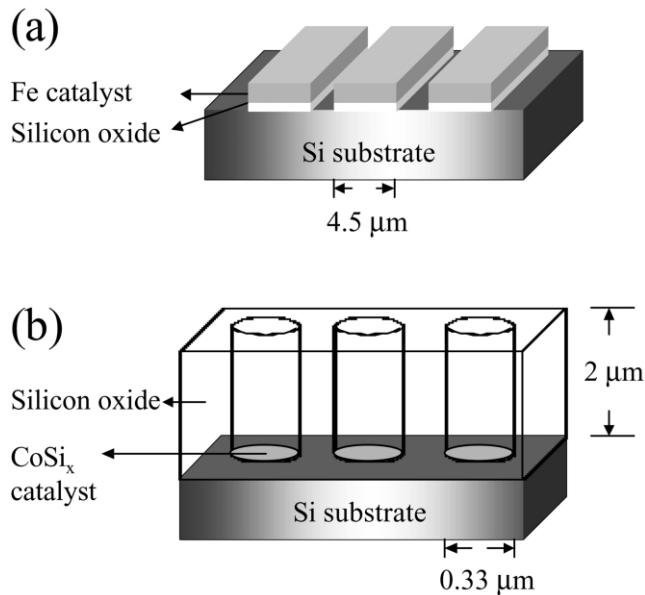


Fig. 1. Schematic diagrams (a) Fe-coated SiO₂ line arrays; (b) SiO₂ hole arrays with CoSi_x on the bottom of the hole.

and holes, as shown in Fig. 1, by a MPCVD system with source gases of CH₄+H₂ or CH₄+H₂+N₂. Two kinds of catalytic films were employed on Si and on the patterned wafers before carbon nanostructures synthesis: (1) Fe film (20 Å) and (2) Co film (75 Å) followed by two-step rapid thermal annealing (RTP) at 600 °C for 60 s and 760 °C for 20 s, under N₂ ambient. The solid-state interaction between Si substrate and Co film causes the formation of CoSi_x phase. Patterned CoSi_x arrays with CoSi_x catalysts at the bottom of the holes were prepared by photolithography of the Si semiconductor process, in which the CoSi_x film is formed by RTP and the self-aligned silicide process (SALICIDE) [16]. CNTs or carbon nano-rods were synthesized as follows. (1) Reduction in H₂ plasma at 0.67 kPa for 10 min at a microwave power of 500 W; (2) introduction of CH₄/H₂ or CH₄/N₂/H₂ process gases at a pressure of 2.13 kPa, and a microwave power of 800 W. Table 1 lists the process conditions and the results. The deposition temperatures were estimated by placing a thermocouple under the substrate holder.

Table 1
Sample designations and corresponding descriptions

Sample	Catalyst	Source gases (sccm)	Time (min)	Temperature (°C)	Morphology
1 ^a	Fe	CH ₄ /H ₂ = 10/100	6	~ 680	Hollow CNTs
2	Fe	CH ₄ /H ₂ /N ₂ = 10//100/100	5	~ 700	Bamboo-like CNTs
3	Fe	CH ₄ /H ₂ = 1/100	30	~ 650	Amorphous conical nano-rods
4	Fe	CH ₄ /H ₂ = 1/100	120	~ 650	Amorphous conical nano-rods
5	CoSi _x	CH ₄ /H ₂ = 1/100	30	~ 650	Amorphous conical nano-rods
6 ^b	CoSi _x	CH ₄ /H ₂ = 10/100	10	~ 680	Hollow CNTs

^a The patterned Si wafer with parallel line arrays.

^b The patterned Si wafer with hole arrays.

The composition gradient of CoSi_x film before nanostructures deposition was examined by Auger electron spectroscopy. Depth profile analysis indicates that the surface compositions are equivalent to CoSi. The morphologies and microstructures of the nanostructures were identified by SEM and TEM. FE properties were evaluated by *I*-*V* measurement at 10⁻⁶ Torr with an electrode-separation of 100 μm.

3. Results and discussion

3.1. Nanostructures morphologies on line arrays and on flat substrate

The process conditions in this study can be divided into two series. The first uses different source gases, either CH₄/H₂ = 10/100 sccm (Sample 1) or CH₄/H₂/N₂ = 10/100/100 sccm gases (Sample 2). The second uses the same source gases but different catalysts, either Fe catalysts (Samples 3 and 4) or CoSi_x catalyst (Sample 5). For the first series, Fig. 2a presents the morphologies of CNTs (Sample 1) on the patterned Si wafers with Fe as catalysts. According to this figure, the CNTs of 18 μm in length are selectively deposited on the Fe-coated line arrays at a deposition rate of 3 μm/min. The CNTs are essentially well-aligned, uniform in size and perpendicular to the substrate. In contrast to Sample 1, Fig. 2b displays the SEM morphology of the well-aligned CNTs of Sample 2 synthesized by adding N₂ gas into CH₄/H₂ gases in the reaction chamber, and indicates decrease in deposition rate (9 μm in length, deposition rate of 1.8 μm/min).

Well-aligned CNTs have been reported elsewhere in Refs. [17–24]. Their growth mechanisms have attracted much interest. The proposed mechanisms include, the preferential etching of CNTs or carbon nano-fibers (CNFs) [17], van der Waals interactions between neighboring CNTs [18]; crowding effect [19], negative bias application [20], electrostatic force effect by plasma, that is, plasma-induced alignment [21], coulomb attraction [22], external applied field [23] and others. Recently, Merkulov et al. proposed a model that explains the alignment process as a result of a feedback mechanism associated with a nonuniform stress (part tensile, part

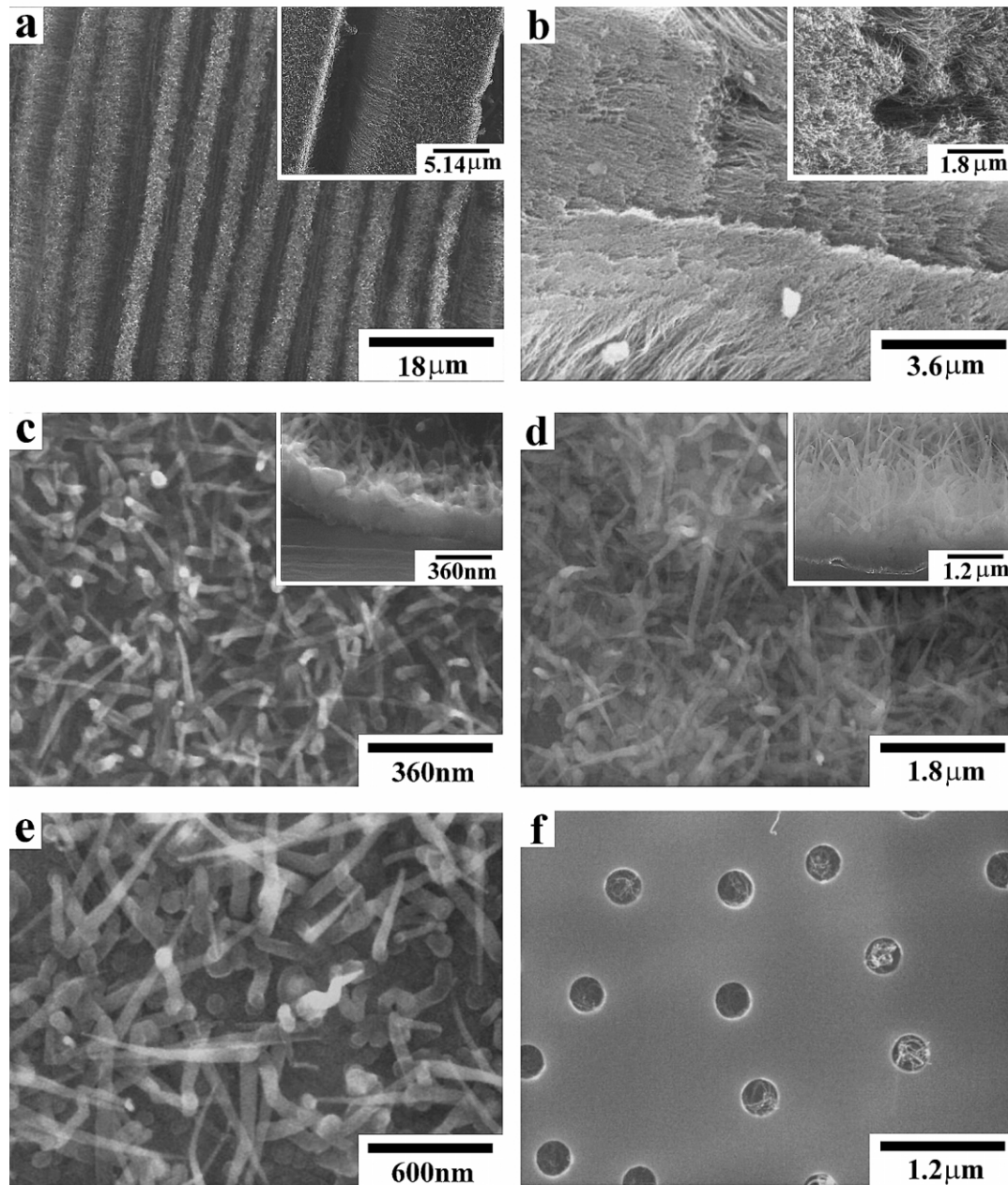


Fig. 2. SEM micrographs (a) top-views of Sample 1 at two magnifications; (b) top-views of CNTs of Sample 2 at two magnifications; (c) top-view and cross-section view of Sample 3; (d) top-view and cross-section view of Sample 4; (e) top-view of Sample 5; (f) top-view of Sample 6.

compressive) that is created across the interface of catalyst particle [24]. Applying the above mechanisms to the present results is interesting. The electrostatic force induced by the plasma can generate highly oriented and fast carbon ions. This promotes the growth of oriented CNTs. However, fluctuation may occur during the synthetic process, in which situation, the crowding of neighboring CNTs due to initially dense catalyst particles dominates the explanations of the alignment

mechanism, and the growth of freestanding CNTs or CNFs could be difficult in this case.

For the second series, in which the source gases are the same but the catalyst materials differ, Fig. 2c and d depict the morphologies of carbon nano-rods synthesized with different deposition times of 30 min and 2 h but with a fixed gas source ratio (CH_4/H_2) and catalyst (Fe), respectively. Notably, randomly oriented nano-rods with cone shape are obtained instead of the aligned

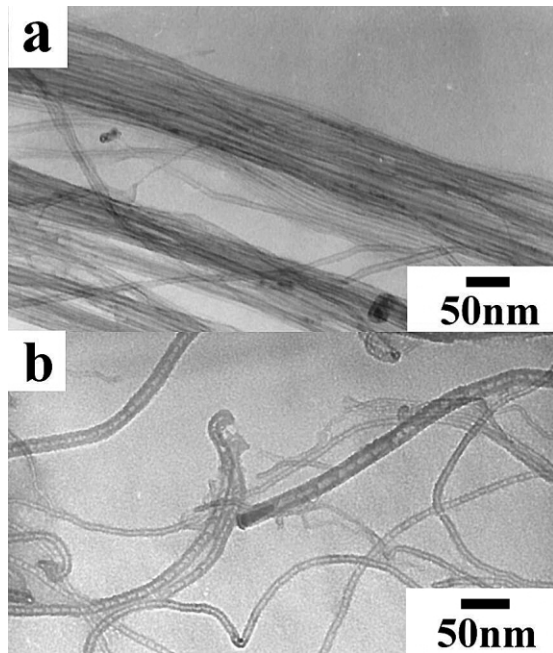


Fig. 3. TEM microstructures (a) hollow CNTs of Sample 1; (b) bamboo-like CNTs of Sample 2.

CNTs as shown in Fig. 2a and b. Increasing deposition time lengthens the nano-rods from 0.6 to 3.6 μm without changing their conical shape. Similarly, cone-shaped carbon nano-rods are obtained under the same process conditions except when the Fe catalysts are replaced by CoSi_x catalysts, as shown in Fig. 2e. In addition, the CoSi_x catalysts increase the deposition rate more than does the Fe catalysts. In summary, carbon nanostructures, such as CNTs or carbon nano-rods, can be controlled by manipulating the compositions and the ratios of the gases, and the catalyst materials.

3.2. Growth of CNTs in the hole arrays

Selective growth of CNTs using CoSi_x catalysts was studied, to develop the CNTs for applications in micro-electronic devices. Fig. 2f shows selective CNTs deposition applied on a patterned Si wafer with hole (aspect ratio = 6) arrays; the CNTs are selectively deposited in the holes. The SEM graph reveals that the selectivity of the process is quite high and the CNTs are wrapped inside the holes with a tube diameter of ~ 15 nm, rather than being well-aligned CNTs as shown in Fig. 2a, under the same process conditions. The possible reason for the wrapping of the CNTs in the holes is the local circular flow of gases in each hole.

3.3. TEM images and the formation mechanisms of the nanostructures

Fig. 3a and b illustrate the microstructures of the CNTs, obtained by TEM for Samples 1 and 2, respec-

tively. Comparing Fig. 3 a and b reveals that bamboo-like CNTs are formed rather than hollow CNTs by adding N_2 to the source gases. The bamboo-like nanotube is a hollow tube that consists of many interior compartments. Mechanisms of formation have been the subject to many debates [25–29]. The precipitations of graphite sheets are formed as a cap on the surface of the catalytic particle, and then these graphite sheets may slide out of the catalytic particle when the accumulated stress reaches a certain value. The above cycle is repeated to yield a series of compartments that become bamboo-like CNTs. The N_2 gas introduction may change the diffusion paths of carbon atoms in the catalyst particles, forming the cap on the catalyst particles. Also, it increases the bending stress of the cap by replacing carbon sites with nitrogen, changing the bonding to pentagonal, heptagonal, or another type. The bending stress of the cap may accumulate beyond the point, at which the cap gradually slides out from the catalyst particle. The formation of the bamboo-like CNTs basically uses the catalyst particle as template for duplicating the caps of the nanotubes.

Fig. 4a and b depict the microstructures of carbon nano-rods, obtained by TEM, using Fe as the catalysts at deposition time of 30 min and 2 h for Sample 3 and Sample 4, respectively. The TEM sample for nano-rods, shown in Fig. 4a, was prepared by ultrasonic dispersion on the grid and in Fig. 4b by mechanical polishing and ion milling. Notably, the nano-rods, shown in both graphs, consist of conical sidewalls and the inner fine channel filled with catalyst material. According to Fig. 4 b, catalysts were embedded in the substrate, signifying a base growth mechanism. The formation of the inside channel in the nano-rod is related to the catalyst, in a manner similar to how the catalyst assists the formation of hollow CNTs. Possible reasons for filling of the inner channel with the catalyst are caused by the capillary force and the suction of the channel under vacuum. A lower carbon concentration ($\text{CH}_4/\text{H}_2 = 0.01$) in the plasma atmosphere favors the formation of a gas-tight channel in the nano-rods. As the nano-rod grows outward, the nano-rod creates a vacuum in the channel to suck liquid catalyst. The carbon atoms continually deposit on the sides of inner channel along the deposition time, the cone shaped nano-rod is thus formed. This is in agreement with production of some voids, by sucking Fe into channel, observed at the interface between Si substrate and Fe catalyst. Notably, most nano-rods at the deposition time of 2 h (Fig. 4b) are not delaminated after mechanical polishing for TEM sample preparation. A stronger chemical Fe–silicide bond may be formed by prolonged heating or deposition. Another significant feature of Fig. 4a and b is that the deposition conditions are the same as in diamond film or diamond like film synthesis, except when the Fe catalyst is applied [30,31]. This feature may open the

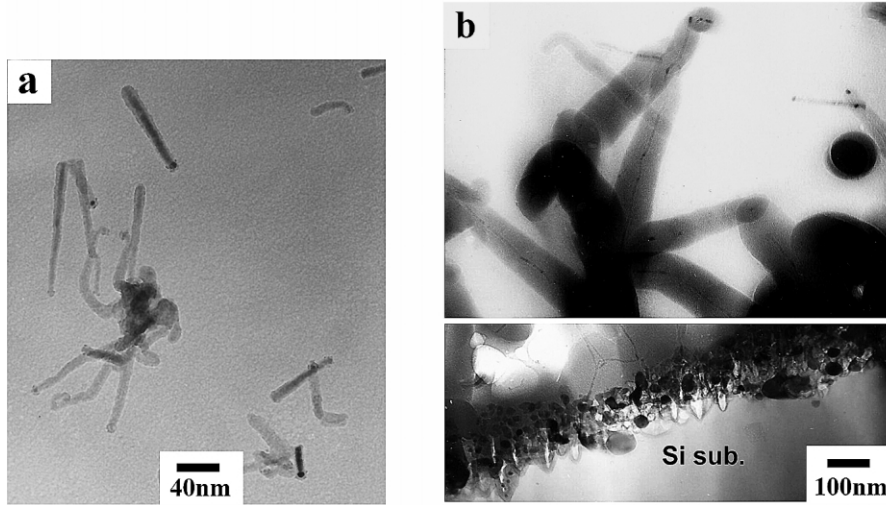


Fig. 4. TEM microstructures of various conical nano-rods (a) top-view of Sample 3; (b) cross-section view of Sample 4.

way to exploring the deposition mechanisms of diamond, CNTs and other nanostructures, all of which made of carbon atoms. The nano-rods could have a structure similar to the diamond-like carbon (DLC) structure. Further study is required.

3.4. Field emission properties

The FE properties of CNTs depend on the geometric enhanced factor (GEF), effective emission sites and

microstructures. The other variables, such as the FE measurement tool, surface contamination, modifications of the surface after testing, and arcing effect are also considered to be crucial [32]. Fig. 5a compares the $J-E$ curves of CNTs prepared with different source gases (Samples 1 and 2). Fig. 5b and c present the corresponding Fowler–Nordheim (F–N) plots for Samples 1 and 2, respectively. The turn-on electric fields at a current density of $1 \mu\text{m}/\text{cm}^2$ are 2.71 and $3.87 \text{ V}/\mu\text{m}$ for Samples 1 and 2, respectively. Also, the current density

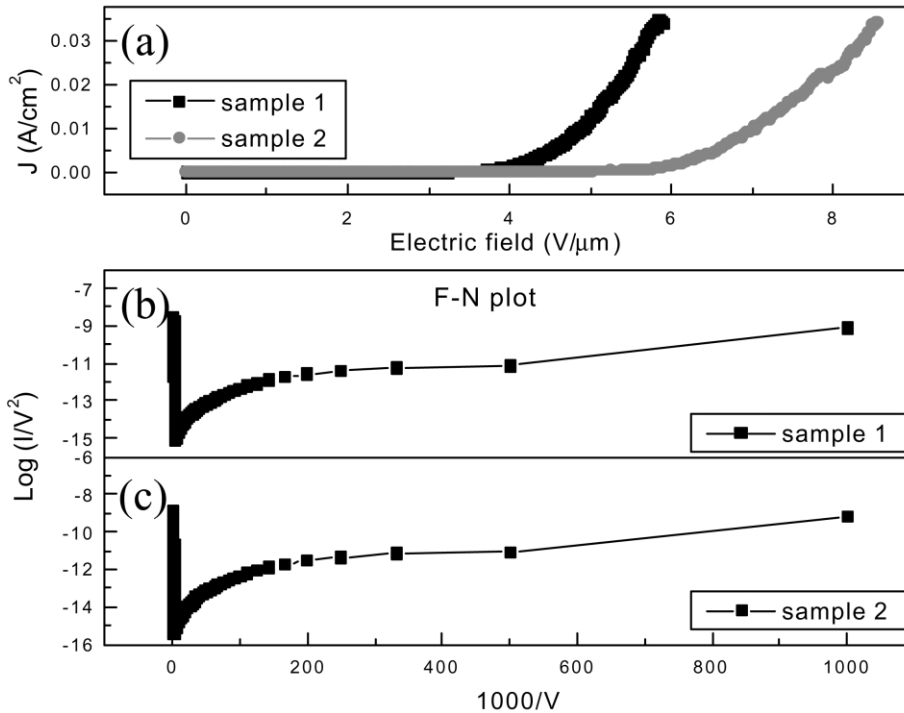


Fig. 5. (a) $J-E$ curves of hollow CNTs and bamboo-like CNTs (Samples 1 and 2); (b) and (c) the corresponding F–N plots of (a).

of 1 mA/cm², required for a flat panel display [33], is obtained at 3.97 and 5.9 V/μm for Samples 1 and 2, respectively. The higher turn-on electric field and lower current density for Sample 2 than for Sample 1 are considered to be due to the bamboo-like structure and greater tube diameter. The GEF of Sample 2 is therefore reduced.

4. Conclusions

This work develops the synthesis processes to selectively deposit different carbon nanostructures, including CNTs and carbon nano-rods, on patterned or un-patterned Si substrates using Fe and CoSi_x as catalysts. Effects of N₂ addition, catalyst materials and carbon concentration on the formation of various nanostructures were studied. The results show that adding nitrogen is crucial to the formation of bamboo-like CNTs. A possible mechanism is also proposed. Various carbon nanostructures, such as the aligned CNTs, the nested CNTs and nano-rods are synthesized by manipulating the carbon and nitrogen concentration in the source gases, the catalyst and the patterned substrate. To the authors' knowledge, this work successfully deposits CNTs in the small hole arrays with a diameter <0.33 μm for the first time. The work has promising application in the fabrication of microelectronic devices.

Acknowledgments

The authors would like to thank the supports of the National Science Council (Contract No.: NSC90-2216-E-009-034, -035 and -040) and the Ministry of Education of Taiwan (Contract No.: 89-E-FA06-1-4).

References

- [1] S. Iijima, *Nature (Lond.)* 354 (1991) 56.
- [2] M.M.J. Treacy, T.W. Ebbesen, J.M. Gibson, *Nature (Lond.)* 381 (1996) 678.
- [3] T.W. Ebbesen, H.J. Lezec, H. Hiura, J.W. Bennett, H.F. Ghaemi, T. Thio, *Nature* 382 (1996) 54.
- [4] W.A. de Heer, W.A. Chatelain, D.A. Ugarte, *Science* 270 (1995) 1179.
- [5] J. Liu, A.G. Rinzler, H. Dai, J.H. Hafner, R.K. Bradley, P.J. Boul, A. Lu, T. Iverson, K. Shelimov, C.B. Huffman, F. Rodriguez-Macias, Y.S. Shon, T.R. Lee, D.T. Colbert, R.E. Smalley, *Science* 280 (1998) 1253.
- [6] H. Dai, J.H. Hafner, A.G. Rinzler, D.T. Rinzler, D.T. Colbert, R.E. Smalley, *Nature* 384 (1996) 147.
- [7] F. Ito, K. Konuma, A. Okamoto, *J. Appl. Phys.* 89 (2001) 8141.
- [8] G. Che, B.B. Lakshmi, E.R. Fisher, C.R. Martin, *Nature* 384 (1996) 147.
- [9] P.G. Collins, A. Zettle, H. Bando, A. Thess, R.E. Smally, *Science* 278 (1997) 100.
- [10] G. Che, B.B. Lakshmi, E.R. Fisher, C.R. Martin, *Nature* 393 (1998) 346.
- [11] Q. Zhao, J.R. Wood, H.D. Wagner, *Appl. Phys. Lett.* 78 (2001) 1748.
- [12] C. Journet, W.K. Maser, P. Bernier, A. Loiseau, M. Lamy de la Chapelle, S. Lefrant, P. Deniered, R. Lee, J.E. Fischer, *Nature* 308 (1997) 756.
- [13] N.R. Franklin, H. Dai, *Adv. Mater.* 12 (2000) 890.
- [14] Y.H. Lee, Y.T. Jang, C.H. Choi, D.H. Kim, C.W. Lee, J.E. Lee, Y.S. Han, S.S. Yoon, J.K. Shin, S.T. Kim, E.K. Kim, B.K. Ju, *Adv. Mater.* 13 (2001) 1371.
- [15] Y.S. Han, J.K. Shin, S.T. Kim, *J. Appl. Phys.* 90 (2001) 5731.
- [16] K.K. Ng, W.T. Lynch, *IEEE Trans. Electron. Devices* ED-34 (1987) 503.
- [17] S.H. Tasi, C.W. Chao, C.L. Lee, H.C. Shih, *Appl. Phys. Lett.* 74 (1999) 3462.
- [18] S. Fan, M.G. Chapline, N.R. Franklin, T.W. Tomblor, A.M. Cassell, H. Dai, *Science* 283 (1999) 512.
- [19] R. Andrews, D. Jacques, A.M. Rao, F. Derbyshire, D. Qian, X. Fan, E.C. Dickey, J. Chen, *Chem. Phys. Lett.* 303 (1999) 467.
- [20] C.H. Lin, H.L. Chang, C.T. Kuo, *Diam. Relat. Mater.* 11 (2002) 922.
- [21] C. Bower, W. Zhu, S. Jin, O. Zhou, *Appl. Phys. Lett.* 77 (2000) 830.
- [22] Y. Avigal, R. Kalish, *Appl. Phys. Lett.* 78 (2001) 2291.
- [23] A. Srivastava, A.K. Srivastava, O.K. Srivastava, *Carbon* 39 (2001) 201.
- [24] V.I. Merkulov, A.V. Melechko, M.A. Guillorn, D.H. Lowndes, M.L. Simpson, *Appl. Phys. Lett.* 79 (2001) 2970.
- [25] Y. Saito, *Carbon* 33 (1995) 979.
- [26] C.J. Lee, J. Park, *Appl. Phys. Lett.* 77 (2000) 3397.
- [27] V.V. Kovalevski, A.N. Safronov, *Carbon* 36 (1998) 963.
- [28] X. Ma, E.G. Wang, *Appl. Phys. Lett.* 78 (2001) 978.
- [29] H.L. Chang, C.H. Lin, C.T. Kuo, *Diam. Relat. Mater.* 11 (2002) 793.
- [30] R. Spitzl, V. Raiko, R. Heiderhoff, H. Gnaser, J. Engemann, *Diam. Relat. Mater.* 4 (1995) 563.
- [31] S.L. Sung, X.J. Guo, K.P. Huang, F.R. Chen, H.C. Shih, *Thin Solid Films* 315 (1998) 345.
- [32] V.I. Merkulov, D.H. Lowndes, L.R. Baylor, S. Kang, *Solid State Electron.* 45 (2001) 949.
- [33] G.A.J. Amarantanga, S.R.P. Silva, *Appl. Phys. Lett.* 68 (1996) 2529.